

缺氧诱导因子-1在兔结膜伤口愈合模型的表达

龚若文, 吴克玲, 左成果, 黄丹平, 林明楷

(眼科学国家重点实验室//中山大学中山眼科中心, 广东 广州 510060)

摘要:【目的】检测缺氧诱导因子-1(HIF-1)在兔结膜伤口愈合模型的表达水平,并研究其在结膜瘢痕形成中的作用。【方法】48只新西兰白兔根据不同观察时间点(术后12 h和1、3、5、7 d以及空白对照组)随机分为6组。对所有实验组动物构建低位结膜瓣,术后观察术区并评估结膜血管化水平。实时荧光定量PCR和蛋白免疫印迹(Western blot)检测术区HIF-1 α 的表达水平,根据病理切片评估术区结膜纤维化水平。【结果】Western Blot结果显示HIF-1 α 蛋白表达水平在术后第3天($P < 0.001$)和第5天($P < 0.001$)均高于空白对照组。在术后不同时间点,HIF-1 α 的mRNA水平的变化趋势与HIF-1 α 的蛋白水平的变化趋势相一致。术后结膜血管化水平与HIF-1 α 的蛋白水平呈正相关关系($r = 0.626$; $P < 0.001$)。此外,术后第3天[(37.88 \pm 6.88)%; $P = 0.006$]、第5天[(47.50 \pm 6.26)%; $P < 0.001$]和第7天[(53.45 \pm 3.78)%; $P < 0.001$]的胶原纤维含量高于空白对照[(23.61 \pm 5.26)%]。【结论】构建兔结膜伤口愈合模型后,HIF-1 α 在兔结膜和Tenon's囊组织存在表达。HIF-1 α 过表达可能促进兔结膜伤口愈合。

关键词:缺氧诱导因子-1;结膜伤口愈合;结膜血管化

中图分类号:R77 **文献标志码:**A **文章编号:**1672-3554(2018)06-0827-08

Expression of Hypoxia Inducible Factor-1 (HIF-1) in a Rabbit Model of Conjunctival Wound Healing

GONG Ruo-wen, WU Ke-ling, ZUO Cheng-guo, HUANG Dan-ping, LIN Ming-kai

(State Key Laboratory of Ophthalmology // Zhongshan Ophthalmic Center, Sun Yat-sen University, Guangzhou 510060, China)

Corresponding to: HUANG Dan-ping, E-mail: hdanp@mail.sysu.edu.cn; LIN Ming-kai, E-mail: linmk@mail.sysu.edu.cn

Abstract: 【Objective】To detect the expression of HIF-1 in a rabbit model of conjunctival wound healing, and to analyze the function of HIF-1 in rabbit conjunctival scar formation. 【Methods】Forty-eight rabbits were separated into six groups based on different postoperative points, including the 12th hour (12H), first day (D1), third day (D3), fifth day (D5), seventh day (D7) after the procedure, with a corresponding blank control (CON). All cases in the experimental groups were surgically prepared with fornix-based conjunctival flaps, and postoperative conjunctival vascularity was observed. At the surgical sites, the expression of HIF-1 α was detected via Western Blot and real-time polymerase chain reaction, and histology was also observed to assess conjunctival fibrosis. 【Results】Western blot analysis indicated that the expression of HIF-1 α protein was significantly higher on D3 ($P < 0.001$) and D5 ($P < 0.001$) in the experimental groups than in the CON group, and the change of the level of HIF-1 α mRNA was consistent with the change of the level of HIF-1 α protein at different postoperative points. Postoperative images presenting conjunctival vascularity were positively correlated with the expression of HIF-1 α protein ($r = 0.626$; $P < 0.001$). Moreover, collagen content in the subconjunctival and Tenon's tissues was markedly elevated on D3 [(37.88 \pm 6.88)%; $P = 0.006$], D5 [(47.50 \pm 6.26)%;

收稿日期:2018-05-03

基金项目:国家自然科学基金(81570846);广东省科技计划项目(303090100501028)

作者简介:龚若文,在读硕士生,研究方向:青光眼、眼整形, E-mail: gongruowen@163.com; 黄丹平,通信作者,博士,主任医师,教授,研究方向:眼整形, E-mail: hdanp@mail.sysu.edu.cn; 林明楷,通信作者,博士,主任医师,教授,研究方向:青光眼, E-mail: linmk@mail.sysu.edu.cn

$P < 0.001$] and D7 [(53.45 ± 3.78)%; $P < 0.001$] in the experimental groups compared to the CON group [(23.61 ± 5.26)%]. 【Conclusion】 HIF-1 α was expressed on rabbit conjunctiva and Tenon's capsule after developing a rabbit model of conjunctival wound healing. In addition, the overexpression of HIF-1 could promote conjunctival wound healing in rabbits.

Key words: hypoxia inducible factor-1; conjunctival wound healing; conjunctival vascularity

[J SUN Yat-sen Univ(Med Sci), 2018, 39(6): 827-834; 872]

Filtration surgery is one of the most common surgical treatments of glaucoma, but there is considerable risk of complication. Bleb scarring is the most evident and it can cause filtration obstruction and even surgery failure. The use of antimetabolites^[1-2] or glucocorticoid^[3] can improve the success rate of filtration surgery, but these medicines have many side effects, including bleb leaks, bleb infections, endophthalmitis, chronic hypotony, corneal epithelial toxicity^[4] and glucocorticoid-associated ophthalmopathy and abnormal physical condition^[5]. The study of postoperative scarring at the molecular level could lead to more effective ways of treating glaucoma. As the main cause of bleb scarring is hyperproliferation of conjunctival fibroblasts^[6], we simplified the experimental glaucoma-filtration-surgery model to a conjunctival wound-healing model to explore conjunctival scarring. Studies have shown there are many crucial growth factors and cytokines, including vascular endothelial growth factor (VEGF)^[7], transforming growth factor (TGF)- β ^[8] and matrix metalloproteinases (MMPs)^[9], participate in postoperative scarring after experimental glaucoma filtration surgery. Specifically, hypoxia inducible factor-1 (HIF-1) is one of the upstream factors of all the factors mentioned above, and it is also the most potent regulator of oxygen homeostasis during tissue repair and wound healing^[10-11]. HIF-1 is a heterodimer composed of an alpha (HIF-1 α) and a beta (HIF-1 β) subunit, which are crucial to regulation of transcriptional activity in a gene array, thereby boosting fibrosis^[11]. To date, there are no studies concerning the impact of HIF-1 on conjunctival wound healing. Numerous studies^[12-14] have documented that the loss of HIF-

1 α leads to poor cutaneous wound vascularity and slower cutaneous wound healing, while the activation of HIF-1 α accelerates wound healing. These findings inspired the present analysis of the role of HIF-1 α in conjunctival wound healing. The purpose of this study is to investigate the expression and potential role of HIF-1 at the surgical site in a rabbit model of conjunctival wound healing.

1 Materials and methods

1.1 Experimental animals

All procedures involving animal experiments followed the National Institutes of Health Guide for the Care and Use of Animals in Research and were approved by the Animal Ethics Committee of Zhongshan Ophthalmic Center, Sun Yat-sen University. Forty-eight adult New Zealand White rabbits, twenty-four males, and twenty-four females, weighing 2.0-3.0 kg, were provided by the Animal Laboratory of Zhongshan Ophthalmic Center, Sun Yat-sen University. All animals were fed ad libitum and housed individually with a 12h/12h light-dark cycle.

1.2 Study design and surgical procedure

The rabbits were randomly divided into six groups (eight in each group, four males, and four females). The groups were based on different postoperative points, including the 12th hour (12H), first day (D1), third day (D3), fifth day (D5), and seventh day (D7), with a corresponding blank control (CON) group. Animals were surgically prepared with conjunctival flaps to imitate the progression of conjunctival wound healing. Pentobarbital sodium (40 mg/kg; Sigma, Santa Clara, CA) was injected intra-

muscularly to induce general anesthesia, and proxymetacaine hydrochloride eye drops (Alcon, Fort Worth, TX) were used to induce local anesthesia. Forty rabbits were prepared with "L-shaped" fornix-based conjunctival flaps in the operative eyes, and subsequent blunt dissection of Tenon's and conjunctiva was done on the surface of the sclera. Another eight rabbits were in the CON group. No anti-scarring medicine was used. Finally, the conjunctiva was closed with 10-0 nylon suture (Alcon). For these forty-eight rabbits, forty of them were sacrificed at 12H, D1, D3, D5, or D7 after surgery, and another eight formed the CON group.

1.3 Western Blot analysis

RIPA lysis buffer (Beyotime, Shanghai, China) and phenylmethanesulfonyl fluoride (Beyotime) were combined 100:1 to extract total protein from the conjunctiva and Tenon's tissue at the surgical sites. All samples were centrifuged at $14,000 \times g$ and $4\text{ }^{\circ}\text{C}$ to obtain protein supernatant. Then, the samples were denatured with SDS-PAGE Sample Loading Buffer, 5X (Beyotime) at $100\text{ }^{\circ}\text{C}$ for 5 min. After denaturation, samples were stored at $-20\text{ }^{\circ}\text{C}$ until use. The samples were separated electrophoretically (Bio-Rad, Hercules, CA) in 8% SDS-PAGE gels (Beyotime), and the proteins were transferred (Bio-Rad) to a polyvinylidene fluoride membrane ($0.45\text{ }\mu\text{m}$; Millipore, Billerica, USA). After blocking in Tris-buffered saline (TBS) containing 0.1% Tween-20 and 5% dry milk for 1 hour at room temperature, the blots were probed with specific antibodies overnight at $4\text{ }^{\circ}\text{C}$: a monoclonal mouse anti-HIF-1 α antibody (NB100-105, Novus, Colorado, USA) diluted 1:250, or a polyclonal rabbit anti- β -actin antibody (4970, Cell Signaling Technology, Boston, MA) diluted 1:1000. After washing with TBS containing 0.1% Tween-20, the blots were incubated with the respective secondary antibodies (Cell Signaling Technology) for 1 hour at room temperature. By using Immobilon Western Chemiluminescent HRP Substrate (Millipore), the specific bands were visualized via Bio-Rad Chemi Doc XRS imaging system (Bio-Rad). Imaging with ImageJ software (Rawak Soft-

ware Inc., Stuttgart, Germany) was performed to quantify the bands, and the protein level of HIF-1 α was expressed as ratio to β -actin level.

1.4 Ribonucleic acid (RNA) preparation and real-time polymerase chain reaction (RT-PCR)

At different postoperative periods, TRIzol Reagent (Invitrogen, MA, USA) was used to extract total RNA from the conjunctiva and Tenon's capsule at the surgical site, and reverse transcription was performed using the PrimeScript RT Master Mix kit (TaKaRa, Kusatsu, Japan), according to the manufacturer's instructions. SYBR Green chemistry (Roche, Basel, Switzerland) was used to quantify the RNA, and the PCR protocol complied with the manufacturer's instructions (one cycle of pre-incubation at $95\text{ }^{\circ}\text{C}$ for 600 s, and forty-five cycles of denaturation at $95\text{ }^{\circ}\text{C}$ for 5 s, anneal at $60\text{ }^{\circ}\text{C}$ for 20 s, and extension at $72\text{ }^{\circ}\text{C}$ for 20 s). The RT-PCR was performed using a real-time PCR system (LightCycler 96 Real-Time PCR System, Roche). In this experiment, the sense and antisense primers (Sangon Biotech, Shanghai, China) were implemented as follows: HIF-1 α sense: 5'-CCA CAG GAC AGT ACA GGA TG-3'; HIF-1 α antisense: 5'-TCA AGT CGT GCT GAA TAA TAC C-3'; β -actin sense: 5'-CCT GTA CGC CAA CAC AGT GC-3'; and β -actin antisense: 5'-ATA CTC CTG CTT GCT GAT CC-3'. The normalized HIF-1 α mRNA level of the CON group was set as 1.0.

1.5 Evaluation of conjunctival vascularity

The appearance of the conjunctiva at the surgical area was observed to examine conjunctival vascularity. Postoperative images were acquired via operating microscope (Leica M844, Wetzlar, Germany), and the technique to quantify conjunctival vascularity was in accordance with that reported by Sumi et al.^[15]. ImageJ software was used to quantitatively evaluate conjunctival vascularity, which was interpreted as the percent pixel coverage of the conjunctival vascularity area.

1.6 Histology

The surgically impacted regions of the rabbit eyes were collected, immediately fixed in 4% parafor-

maldehyde overnight at room temperature and embedded in paraffin wax. Tissues were sectioned at 5 μm thickness. Once the resulting sections were deparaffinized, they were stained with hematoxylin and eosin or Masson's Trichrome. The slides were analyzed via light microscopy. Additionally, the slides stained with Masson's Trichrome were observed to examine collagen content. ImageJ software was used to quantitatively evaluate collagen content, which was interpreted as the percent pixel coverage of collagen area.

1.7 Statistical analysis

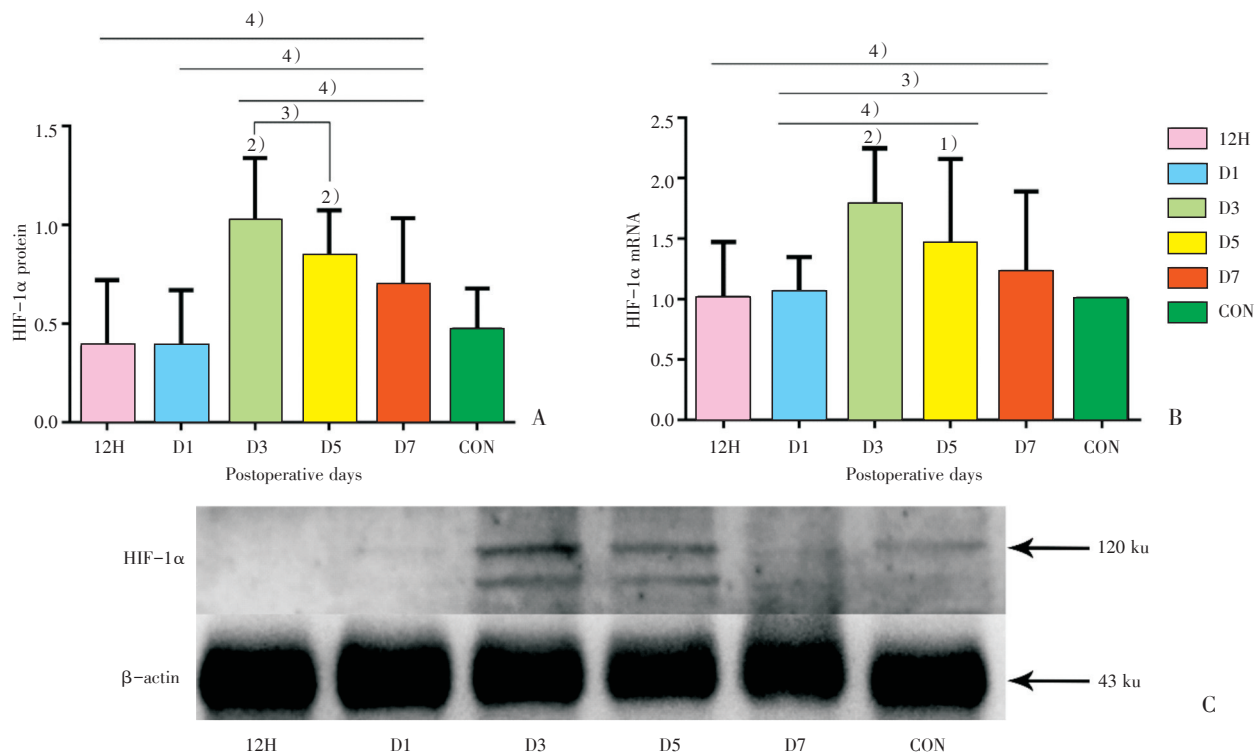
All experimental data were analyzed using SPSS software (version 22.0, IBM SPSS Statistics, IBM Corporation, Chicago, IL), and the results were presented as the mean \pm S.D. When comparisons were made for five or six groups, one-way analysis of variance (ANOVA) was used. Dunnett *t* test was used for comparisons between the experimental and CON

groups. Further multiple comparisons among all the experimental groups were performed with Dunnett T3 test. Moreover, the Pearson coefficient was applied for bivariate correlations. For all tests, statistical analyses were two tailed, and *P* values less than 0.05 indicated statistical significance.

2 Results

2.1 The expression of HIF-1 α

Western Blot analysis (Fig.1C) indicated that the expression of HIF-1 α protein in rabbit conjunctival scar was the highest on D3 and gradually decreased thereafter. The expression of HIF-1 α protein was statistically different between the experimental (12H, D1, D3, D5, D7) and CON groups ($F = 18.586; P < 0.001$). Further comparisons showed that the expression of HIF-1 α protein was significantly



A: Analysis of gray value of relevant Western Blot bands ($n = 8$ /each group); B: analysis of HIF-1 α mRNA level in the experimental groups and CON group ($n = 8$ /each group); C: band of Western Blot. Compared with CON, 1) $P < 0.05$, 2) $P < 0.01$; multiple comparisons among operation groups at different points, 3) $P < 0.05$, 4) $P < 0.01$. For the expression of HIF-1 α protein, *t* values of the comparisons between the experimental (12H, D1, D3, D5, D7) and CON groups were 0.176, 0.203, 10.141, 4.818 and 2.113. For the expression of HIF-1 α mRNA, *t* values of the comparisons between the experimental (12H, D1, D3, D5, D7) and CON groups were < 0.001 , 0.004, 4.470, 2.201 and 0.511.

Fig.1 Expression of HIF-1 α in the experimental groups and CON group

higher in the D3 ($P < 0.001$) and D5 ($P < 0.001$) groups than in the CON group. There were no significant differences between the 12H ($P = 0.863$), D1 ($P = 0.842$) or D7 ($P = 0.053$) and the CON groups (Fig.1A).

Also, the expression of HIF-1 α mRNA was statistically different between the experimental (12H, D1, D3, D5, D7) and CON groups ($F = 5.212$; $P < 0.001$). Further comparisons showed that the expression of HIF-1 α mRNA was significantly higher in the D3 ($P < 0.001$) and D5 groups ($P = 0.045$) than in the CON group. There were no significant differences between the 12H ($P > 0.999$), D1 ($P = 0.997$) or D7 ($P = 0.617$) and the CON groups (Fig.1B). In addition, changes in the HIF-1 α mRNA levels were consistent with HIF-1 α protein levels at different postoperative timepoints (Fig.1A, Fig.1B).

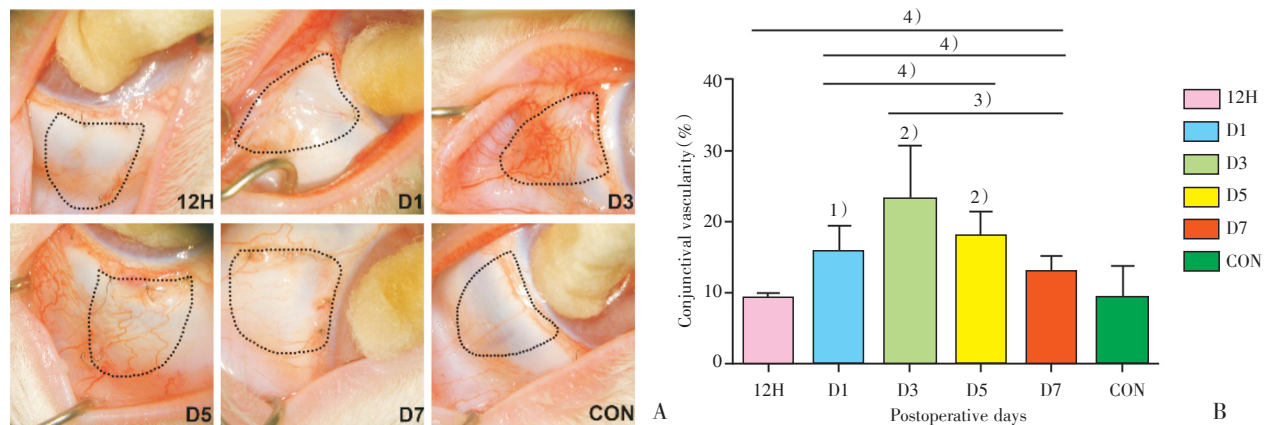
2.2 Conjunctival vascularity of the surgical sites

Conjunctival vascularity became increasingly more severe until D3 and then was relieved after this point (Fig.2A). The results from the evaluation of conjunctival vascularity demonstrated that conjunctival vascularity was most severe on D3 and gradually decreased after this point. The percentage of conjunctival vascularity area was statistically different be-

tween the experimental (12H, D1, D3, D5, D7) and CON groups ($F = 10.375$; $P < 0.001$), and further comparisons showed that the percentage of conjunctival vascularity area was much higher in the D1 [$(15.78 \pm 3.56)\%$; $P = 0.024$], D3 [$(23.21 \pm 7.33)\%$; $P < 0.001$] and D5 groups [$(18.08 \pm 3.32)\%$; $P = 0.001$] than in the CON group [$(9.26 \pm 4.59)\%$]. There were no significant differences between the 12H [$(9.09 \pm 0.72)\%$; $P > 0.999$] or D7 [$(12.84 \pm 2.30)\%$; $P = 0.380$] and CON groups (Fig. 2B). Additionally, conjunctival vascularity was positively correlated with the expression of HIF-1 α ($r = 0.626$; $P < 0.001$).

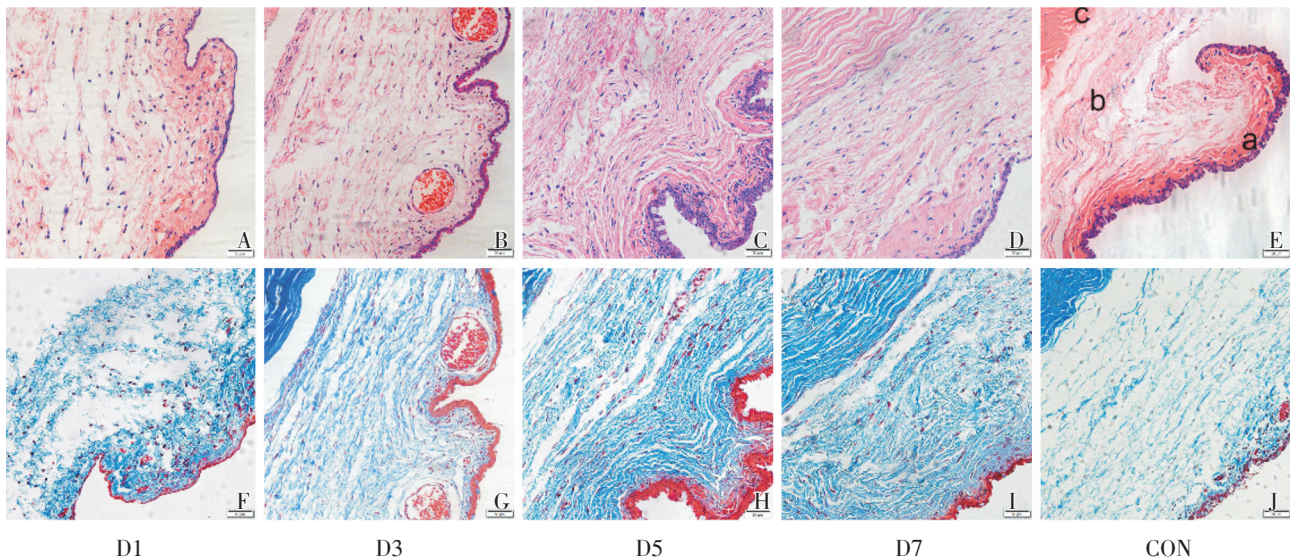
2.3 Histological characteristics of the surgical sites

Hematoxylin and eosin staining displayed the structure of the subconjunctival and Tenon's tissues (Fig.3). Subepithelial connective tissues were loosely arranged in the CON group and on D1 in the experimental groups but gradually increased on D3 and were densely arranged on D5 and D7 (Fig.3A-E). Masson's Trichrome staining revealed the collagen content at the surgical site (Fig.3F-J). The percentage of collagen area was statistically different between the experimental (D1, D3, D5, D7) and



A: Conjunctival appearance of surgical sites between the CON and experimental groups. Conjunctival vascularity was increasingly more severe until D3 and gradually relieved thereafter. B: Percent pixel coverage of conjunctival vascularity showed that conjunctival vascularity was most evident on D3 ($n = 8$ /each group). Compared with CON, 1) $P < 0.05$, 2) $P < 0.01$. Multiple comparisons among operation groups at different points, 3) $P < 0.05$, 4) $P < 0.01$. t values of the comparisons between the experimental (12H, D1, D3, D5, D7) and CON groups were < 0.001 , 2.531, 8.218, 4.140, and 0.907.

Fig.2 Conjunctival vascularity of the surgical sites



Subepithelial connective tissues were loosely arranged in the CON group (E) and on D1 (A), slightly increased on D3 (B), and densely arranged on D5 (C) and D7 (D) ($n = 8$ /each group). Masson's Trichrome staining revealed that the collagen content at the surgical site increased markedly on D3 (G), D5 (H) and D7 (I), while there was no evident increase in collagen on D1 (F) compared to the CON group (J) ($n = 8$ /each group). t values of the comparisons between the experimental (D1, D3, D5, D7) and CON groups were 2.083, 3.234, 6.088 and 8.551. Scale bar, 50 μm . (A: conjunctival epithelium; B: subconjunctiva; C: sclera).

Fig.3 Hematoxylin and eosin staining displayed the subconjunctival and Tenon's structure

CON groups ($F = 20.115$; $P < 0.001$), and further comparisons showed that the percentage of collagen area was markedly elevated in the D3 [$(37.88 \pm 6.88)\%$; $P = 0.006$, D5 ($47.50 \pm 6.26)\%$; $P < 0.001$] and D7 [$(53.45 \pm 3.78)\%$; $P < 0.001$] groups compared to the CON group [$(23.61 \pm 5.26)\%$]. There was no significant difference between D1 [$(33.80 \pm 7.86)\%$; $P = 0.056$] group compared to the CON group.

3 Discussion

Glaucoma is the leading cause of irreversible blindness worldwide, and glaucoma filtration surgery remains the gold standard for controlling intraocular pressure (IOP) when medication and/or laser surgery have proven insufficient^[16-17]. Scar formation at the surgical site may lead to obstruction of aqueous flow and filtration failure. Therefore, it is necessary to study postoperative scarring at the molecular level to identify a new target for the modulation of postopera-

tive wound healing.

We selected the rabbit model of conjunctival wound healing owing to its feasibility in performing glaucoma filtration surgery. Since the main cause of bleb scarring is hyperproliferation of conjunctival fibroblasts^[6], and because the modulation of fibroblast proliferation, differentiation, extracellular matrix production, and apoptosis are very promising to conjunctival wound healing^[18], we simplified the experimental glaucoma-filtration-surgery model to a conjunctival wound-healing model to explore conjunctival scarring.

As the most hypoxia-sensitive factor, HIF-1 is considered an important determinant of healing outcomes^[10-11]. Although its stabilization and inhibition have therapeutic potential in the regulation of wound healing^[19], it is unknown whether HIF-1 plays a significant role in conjunctival wound healing. To our best knowledge, this is the first study concerning the expression of HIF-1 in conjunctival scarring.

In the present study, the expression of HIF-1 α

in the rabbit model of conjunctival wound healing was the highest in D3, which is consistent with the timeline of oxygen availability during tissue repair^[10]. HIF-1 α degrades rapidly under normoxia and is continuously stabilized under hypoxia^[10-11]. Hypoxia tends to occur in the early stage of wound healing, then HIF-1 will begin regulating a series of wound-healing phases. These explanations could account for the highest expression of HIF-1 α found on D3. We speculate that the significantly higher postoperative expression of HIF-1 α stems from the extensive damage to the Tenon's tissues, which not only caused the disruption in conjunctival vasculature, thereby damaging oxygen delivery, but also promoted the recruitment of inflammatory cells to the surgical site, thus exacerbating oxygen consumption. The dwindling concentration of oxygen reduced the degradation of HIF-1 α , as it is the most sensitive to hypoxia. The resulting accumulation of HIF-1 α aids in the subsequent progression of conjunctival wound healing.

Moreover, conjunctival vascularity is an indispensable factor in the assessment of postoperative filtering blebs^[20-22]. Marked bleb scarring and vascularization were observed in all participants who underwent glaucoma surgery^[23]. Increased vascularity was observed in the scarring filtering blebs^[24]. An association between increased maximum bleb vascularity and higher IOP at the fourth postoperative month was observed^[25]. Thus, the level of rabbit conjunctival vascularity could show conjunctival scarring to some extent. Our study indicated that the change in conjunctival vascularity was similar to the trend in the expression of HIF-1 α protein in the rabbit model of conjunctival wound healing, and the level of conjunctival vascularity was positively correlated with the expression of HIF-1 α protein. We speculate that an association between HIF-1 α and rabbit conjunctival vascularity might indicate the prominent role of HIF-1 in conjunctival scarring.

Our results also revealed that the collagen con-

tent at the ocular surgical site had increased significantly within the D3, D5, and D7 groups. As the highest expression of HIF-1 α in the rabbit conjunctival scar was found in D3, we speculate that the hyperexpression of HIF-1 may promote conjunctival wound healing in rabbits. Our previous experiments indicate that the down-regulation of HIF-1 α not only attenuates the overproduction of vascular endothelial growth factor (VEGF) and intercellular adhesion molecule-1 (ICAM-1) but also alleviates choroidal neovascularization or retinal neovascularization^[26-27]. Furthermore, another study demonstrated increased collagen synthesis of keloid fibroblasts under hypoxia compared to that under normoxia^[28]. As a result, we speculate that conjunctival dissection could cause severe inflammation at surgical site and the disruption in conjunctival vasculature, which exacerbates hypoxia and ischemia. This, in turn, elevates the expressions of pro-scarring factors, including HIF-1 α , and eventually accelerates conjunctival neovascularization and conjunctival scarring.

While this study offers promising results concerning the impact of HIF-1 on conjunctival wound healing, it has some limitations. To begin with, this is a rabbit model of conjunctival scarring, which cannot exactly reflect conjunctival wound healing in human eyes. Besides, the intervention of the expression of HIF-1 should also be taken into account, thereby clarifying our results.

In conclusion, this study found that the hyperexpression of HIF-1 may promote conjunctival wound healing in rabbits, including a positive correlation with conjunctival vascularity. The exploration of HIF-1 expression in a rabbit model of conjunctival wound healing could create a solid foundation for the function of HIF-1 signal pathways in wound healing after filtration surgery. Therefore, this study represents the first step toward developing a novel therapeutic target for modulating postoperative scarring in filtration surgery, which can potentially elevate the surgical success rate and deter the progression of glaucoma.

References

- [1] Chen CW, Huang HT, Bair JS, et al. Trabeculectomy with simultaneous topical application of mitomycin-C in refractory glaucoma [J]. *J Ocul Pharmacol*, 1990, 6(3): 175-182.
- [2] Kitazawa Y, Taniguchi T, Nakano Y, et al. 5-Fluorouracil for trabeculectomy in glaucoma [J]. *Graefes Arch Clin Exp Ophthalmol*, 1987, 225(6): 403-405.
- [3] Hogewind BF, Pijl B, Hoyng CB, et al. Purified triamcinolone acetonide as antifibrotic adjunct in glaucoma filtering surgery [J]. *Graefes Arch Clin Exp Ophthalmol*, 2013, 251(4): 1213-1218.
- [4] Hollo G. Wound healing and glaucoma surgery: modulating the scarring process with conventional antimetabolites and new molecules [J]. *Dev Ophthalmol*, 2012, 50(1): 79-89.
- [5] Harris E, Tiganescu A, Tubeuf S, et al. The prediction and monitoring of toxicity associated with long-term systemic glucocorticoid therapy [J]. *Curr Rheumatol Rep*, 2015, 17(6): 513-521.
- [6] Lim DH, Kim TE, Kee C. Evaluation of adenovirus-mediated down-regulation of connective tissue growth factor on postoperative wound healing after experimental glaucoma surgery [J]. *Curr Eye Res*, 2016, 41(7): 951-956.
- [7] Li Z, Van Bergen T, Van de Veire S, et al. Inhibition of vascular endothelial growth factor reduces scar formation after glaucoma filtration surgery [J]. *Invest Ophthalmol Vis Sci*, 2009, 50(11): 5217-5225.
- [8] Cordeiro MF, Gay JA, Khaw PT. Human anti-transforming growth factor-beta2 antibody: a new glaucoma anti-scarring agent [J]. *Invest Ophthalmol Vis Sci*, 1999, 40(10): 2225-2234.
- [9] Wong TT, Mead AL, Khaw PT. Matrix metalloproteinase inhibition modulates postoperative scarring after experimental glaucoma filtration surgery [J]. *Invest Ophthalmol Vis Sci*, 2003, 44(3): 1097-1103.
- [10] Nauta TD, van Hinsbergh VW, Koolwijk P. Hypoxic signaling during tissue repair and regenerative medicine [J]. *Int J Mol Sci*, 2014, 15(11): 19791-19815.
- [11] Hong WX, Hu MS, Esquivel M, et al. The Role of Hypoxia-Inducible Factor in Wound Healing [J]. *Adv Wound Care (New Rochelle)*, 2014, 3(5): 390-399.
- [12] Sunkari VG, Lind F, Botusan IR, et al. Hyperbaric oxygen therapy activates hypoxia-inducible factor 1 (HIF-1), which contributes to improved wound healing in diabetic mice [J]. *Wound Repair Regen*, 2015, 23(1): 98-103.
- [13] Jing L, Li S, Li Q. Akt/hypoxia-inducible factor-1alpha signaling deficiency compromises skin wound healing in a type 1 diabetes mouse model [J]. *Exp Ther Med*, 2015, 9(6): 2141-2146.
- [14] Duscher D, Maan ZN, Whittam AJ, et al. Fibroblast-Specific Deletion of Hypoxia Inducible Factor-1 Critically Impairs Murine Cutaneous Neovascularization and Wound Healing [J]. *Plast Reconstr Surg*, 2015, 136(5): 1004-1013.
- [15] Sumi T, Yoneda T, Fukuda K, et al. Development of automated conjunctival hyperemia analysis software [J]. *Cornea*, 2013, 32 Suppl 1: S52-59.
- [16] Lukowski ZL, Min J, Beattie AR, et al. Prevention of ocular scarring after glaucoma filtering surgery using the monoclonal antibody LT1009 (Sonepcizumab) in a rabbit model [J]. *J Glaucoma*, 2013, 22(2): 145-151.
- [17] Min J, Lukowski ZL, Levine MA, et al. Prevention of ocular scarring post glaucoma filtration surgery using the inflammatory cell and platelet binding modulator saratin in a rabbit model [J]. *PLoS One*, 2012, 7(4): e35627.
- [18] Zada M, Pattamatta U, White A. Modulation of Fibroblasts in Conjunctival Wound Healing [J]. *Ophthalmology*, 2018, 125(2): 179-192.
- [19] Ruthenborg RJ, Ban JJ, Wazir A, et al. Regulation of wound healing and fibrosis by hypoxia and hypoxia-inducible factor-1 [J]. *Mol Cells*, 2014, 37(9): 637-643.
- [20] Klink T, Schrey S, Elsesser U, et al. Interobserver variability of the Wurzberg bleb classification score [J]. *Ophthalmologica*, 2008, 222(6): 408-413.
- [21] Wells AP, Crowston JG, Marks J, et al. A pilot study of a system for grading of drainage blebs after

(下转第872页 to page 872)